

Neutral pion photoproduction on deuterium in baryon chiral perturbation theory to order q^4

S.R. Beane¹, V. Bernard², T.-S.H. Lee³
Ulf-G. Meißner⁴, U. van Kolck⁵

¹*Department of Physics, Duke University, Durham, NC 27708, USA*
and
Department of Physics, University of Maryland, College Park, MD 20742, USA
E-mail address: sbeane@fermi.umd.edu

²*Laboratoire de Physique Théorique*
Université Louis Pasteur, F-67037 Strasbourg Cedex 2, France
E-mail address: bernard@crnhp4.in2p3.fr

³*Physics Division, Argonne National Laboratory, Argonne, IL 60439, USA*
E-mail address: lee@phy.anl.gov

⁴*Institut für Kernphysik, Forschungszentrum Jülich, D-52425 Jülich, Germany*
E-mail address: Ulf-G.Meissner@kfa-juelich.de

⁵*Department of Physics, University of Washington, Seattle, WA 98195-1560, USA*
E-mail address: vankolck@phys.washington.edu

Abstract

Threshold neutral pion photoproduction on the deuteron is studied in the framework of baryon chiral perturbation theory beyond next-to-leading order in the chiral expansion. To fourth order in small momenta, the amplitude is finite and a sum of two- and three-body interactions with no undetermined parameters. With accurate theoretical and experimental input from the single nucleon sector for the proton amplitude, we investigate the sensitivity of the threshold cross section to the elementary $\gamma n \rightarrow \pi^0 n$ amplitude. A precise measurement of the threshold cross section for $\gamma d \rightarrow \pi^0 d$ is called for.

PACS nos.: 25.20.Lj , 12.39.Fe

1 Introduction

One of the major goals in nuclear physics is the understanding of isospin symmetry violation related to the light quark mass difference $m_u - m_d$ and virtual photon effects. Although the light quark mass ratio deviates strongly from unity, $m_d/m_u \sim 2$ [1] and one thus could expect sizeable isospin violation, such effects are effectively masked since $m_d - m_u \ll \Lambda$, with Λ the scale of the strong interactions (which can be chosen to be $4\pi F_\pi$ or 1 GeV or the mass of the ρ). To assess the isospin violation through quark mass differences, precise measurements and accurate calculations are mandatory. As pointed out by Weinberg a long time ago [2], systems involving nucleons can exhibit such effects to leading order in contrast to the suppression in purely pionic processes due to G-parity. Pion-nucleon scattering or neutral pion photoproduction are best suited for such investigations since a large body of (precise) data exists for various isospin channels. While there is still some discrepancy about the low-energy π^-p elastic scattering data, very precise neutral pion photoproduction experiments have been performed over the last few years at MAMI [3] and SAL [4]. Together with the new data on $\gamma p \rightarrow \pi^+n$, a sensitive test of isospin symmetry could be performed if one would have information on the elementary neutron amplitude $\gamma n \rightarrow \pi^0n$. This amplitude can only be inferred indirectly from reactions involving few-nucleon systems like the deuteron or ^3He . In this paper, we concentrate on coherent neutral pion production off deuterium in the threshold region and study the sensitivity of the deuteron electric dipole amplitude E_d to the elementary neutron amplitude, $E_{0+}^{\pi^0n}$. The framework to do this is baryon chiral perturbation theory, which is reviewed in great detail in Ref.[5]. It is the effective field theory of the standard model at energies below 1 GeV and allows one to explore in a systematic fashion the strictures of the spontaneously and explicitly broken chiral symmetry underlying the fundamental color gauge theory of the strong interactions, QCD. While originally formulated for the Goldstone boson sector, the machinery can be extended straightforwardly to include single-baryon processes, treating the baryons as very heavy, static sources [6][7]. In few-nucleon systems, a complication arises due to the existence of shallow nuclear bound states [8] and the related infrared singularities in Feynman diagrams evaluated in the static approximation. One way to overcome this is to adapt the rules and use chiral perturbation theory to calculate an effective potential, which consists of the sum of all A -nucleon irreducible graphs [9]. The S-matrix, which of course includes all reducible contributions, is then obtained through iteration by solving a Lippmann-Schwinger equation. Several generic features of nuclear physics, in particular the relative strengths of two- and few-body forces [8][10][11] or the dominance of soft-pion exchange currents [12], have been shown to arise naturally in this approach. For calculating scattering processes involving light nuclei, Weinberg [13] proposed to use chiral perturbation theory to generate the irreducible kernel and combine these with very accurate phenomenological external nuclear wave functions. Although nuclear wave functions are calculable in chiral perturbation

theory [10], they have not yet been determined with the accuracy matching that of the phenomenological models. Therefore, we use the input from the successful phenomenological boson-exchange potentials which differ mostly in their short-range interaction parts. Using a large variety of these potentials allows one to assess to which degree of accuracy one is sensitive to the chiral symmetry constraints used in determining the irreducible scattering kernel.

In this paper, we consider pion photoproduction on the deuteron at threshold extending the previous work by Beane et al.[14]. We calculate the invariant threshold amplitude to fourth order in small momenta and/or pion masses. This is mandated by the fact that only to this order in the chiral expansion one can achieve a satisfactory description of the elementary process $\gamma p \rightarrow \pi^0 p$ [15][16]. As already stressed in Ref.[14], to third order in small momenta, the interaction kernel for neutral pion photoproduction off the deuteron has no undetermined parameters. Unfortunately, although the same is true in the single nucleon sector, evidently the amplitude there converges slowly at best and thus the single-scattering contribution was treated as phenomenological input. Since that paper was published, the situation has considerably improved and we are now in the position to consistently include the predictions for the single-nucleon sector. In particular, the precise $\mathcal{O}(q^4)$ (where q is a generic symbol for a small momentum or meson mass) chiral perturbation theory calculation [15][16] predicts a very large neutron electric dipole amplitude, larger in magnitude than the corresponding proton one. As we will show, to fourth order in small momenta the interaction kernel can still be given entirely in terms of known parameters, and thus we will be able to calculate the sensitivity of the threshold cross section to the elementary neutron- π^0 amplitude. We mention that charged pion photoproduction at threshold has been calculated accurately (to four orders) in chiral perturbation theory [17].

Since neutral pion photoproduction has already been studied extensively in more conventional nuclear approaches based e.g. on meson-exchange models (see e.g. refs.[18]–[21]), it is worth emphasizing why we use chiral perturbation theory here. As first stressed by Weinberg [13], chiral perturbation theory allows one to *systematically* construct the many-body interactions between nucleons, pions and photons following the power counting rules. For example, in the case of elastic pion-deuteron scattering the phenomenologically dominant rescattering contribution was shown to be the leading three-body interaction in the chiral expansion thus leading to deeper theoretical insight. Here, the phenomenological approaches to the single neutral pion production amplitude off protons based on Born terms are at variance with the data by many standard deviations quite in contrast to chiral perturbation theory. To tackle the problem of how sensitively the deuteron threshold cross section depends on the elementary neutron- π^0 amplitude can therefore only be addressed in a framework which allows one to systematically include and order the various contributions arising from single and multiple scattering processes. It goes without saying that this approach is only useful for the threshold region. We remark

that contributions from the Δ -isobar are encoded in some of the low-energy constants appearing in the single scattering matrix elements.

This paper is organized as follows. In section 2 we briefly review the effective Lagrangian underlying the calculation and the standard power counting formulas. In section 3 the calculation of the various contributions to the threshold S-wave amplitude is outlined. Section 4 contains the results and discussions thereof. The appendices include our conventions and give some more details on the calculations.

2 Effective field theory

In this section, we briefly discuss the effective chiral Lagrangian underlying our calculations and the corresponding power counting. For more details we refer to the review [5] and to the paper by Beane et al.[14].

At low energies, the relevant degrees of freedom are hadrons, in particular the Goldstone bosons linked to the spontaneous symmetry violation. We consider here the two flavor case and thus deal with the triplet of pions, collected in the matrix $U(x) = \xi^2(x)$. It is straightforward to build an effective Lagrangian to describe their interactions, called $\mathcal{L}_{\pi\pi}$. This Lagrangian admits a dual expansion in small (external) momenta and quark (meson) masses as detailed below. Matter fields such as nucleons can also be included in the effective field theory based on the familiar notions of non-linearly realized chiral symmetry. These pertinent effective Lagrangian splits into two parts, $\mathcal{L}_{\pi N}$ and \mathcal{L}_{NN} , with the first (second) one consisting of terms with exactly one (two) nucleon(s) in the initial and the final state. Terms with more nucleon fields are of no relevance to our calculation. The pertinent contributions to neutral pion photoproduction at threshold are organized according to the standard power counting rules, which for a generic matrix element involving the interaction of any number of pions and nucleons can then be written in the form

$$\mathcal{M} = q^\nu \mathcal{F}(q/\mu), \quad (1)$$

where μ is a renormalization scale, and ν is a counting index, i.e. the chiral dimension of any Feynman graph. ν is, of course, intimately connected to the chiral dimension d_i which orders the various terms in the underlying effective Lagrangian (for details, see [5]). For processes with the same number of nucleon lines in the initial and final state (A), one finds[8]

$$\begin{aligned} \nu &= 4 - A - 2C + 2L + \sum_i V_i \Delta_i \\ \Delta_i &\equiv d_i + n_i/2 - 2. \end{aligned} \quad (2)$$

where L is the number of loops, V_i is the number of vertices of type i , d_i is the number of derivatives or powers of M_π which contribute to an interaction of type i with n_i nucleon

fields, and C is the number of separately connected pieces. This formula is important because chiral symmetry places a lower bound: $\Delta_i \geq 0$. Hence the leading *irreducible* graphs are tree graphs ($L = 0$) with the maximum number C of separately connected pieces, constructed from vertices with $\Delta_i = 0$. In the presence of an electromagnetic field, this formula is slightly modified. Photons couple via the electromagnetic field strength tensor and by minimal substitution. This has the simple effect of modifying the lower bound on Δ_i to $\Delta_i \geq -1$, and of introducing an expansion in the electromagnetic coupling, e . Throughout, we work to first order in e , with one exception to be discussed below. In what follows, we will work within the one-loop approximation to order q^4 (notice that we refer here to the chiral dimension used to organize the various terms in the calculation of the single-nucleon photoproduction amplitudes), which extends the $\mathcal{O}(q^3)$ calculation of ref.[14]. Such a higher order calculation is mandated by the fact that to order q^3 the single-nucleon neutral pion photoproduction amplitudes are too inaccurate. Furthermore, one would like to see how big the corrections to the leading order three-body interactions calculated in ref.[14] are. In terms of the counting index ν , in ref.[14] all terms with $\nu = 4 - 3A = -2$ and $\nu = 5 - 3A = -1$ were included. We go one order further, i.e. we add *all* terms with $\nu = 6 - 3A = 0$ (remember that $A = 2$ and we have exactly one photon coupling with $\Delta_i = -1$). Consequently, the effective Lagrangian consists of the following pieces:

$$\mathcal{L}_{\text{eff}} = \mathcal{L}_{\pi\pi}^{(2)} + \mathcal{L}_{\pi N}^{(1)} + \mathcal{L}_{\pi N}^{(2)} + \mathcal{L}_{\pi N}^{(3)} + \mathcal{L}_{\pi N}^{(4)} + \mathcal{L}_{NN}^{(0)} + \mathcal{L}_{NN}^{(1)}, \quad (3)$$

where the index (i) gives the chiral dimension d_i (number of derivative and/or meson mass insertions). The form of $\mathcal{L}_{\pi\pi}^{(2)} + \mathcal{L}_{\pi N}^{(1)}$ is standard. The terms from $\mathcal{L}_{\pi N}^{(3)} + \mathcal{L}_{\pi N}^{(4)}$ contributing to the single-nucleon photoproduction amplitudes are given in ref.[15]. Concerning the terms from $\mathcal{L}_{\pi N}^{(2)}$ and $\mathcal{L}_{NN}^{(1)}$, we will discuss the pertinent ones below.¹ With these at hand, we have to calculate tree and loop graphs for the single-scattering amplitude and tree graphs with exactly one insertion from $\mathcal{L}_{\pi N}^{(2)}$ for the three-body interactions between pions, nucleons and photons as well as tree graphs with one insertion from $\mathcal{L}_{NN}^{(1)}$. As we will show later, the only new coupling constants appearing at $\mathcal{O}(q^4)$ are related to the single-nucleon sector and have already been determined in refs.[15][16]. After these general remarks, let us now turn to the actual calculations.

3 Anatomy of the calculation

In this section, we outline how the various contributions to the electric dipole amplitude E_d are calculated. The pertinent details are relegated to the appendices, including our conventions and definitions of the S-matrix.

¹Of course, terms from $\mathcal{L}_{\pi N}^{(2)}$ also appear in the single nucleon calculation of refs.[15][16] and from $\mathcal{L}_{NN}^{(1)}$ in the nuclear force calculation of ref.[11].

3.1 Threshold cross section

Consider the reaction $\gamma(k) + d(p_1) \rightarrow \pi^0(q) + d(p_2)$ in the threshold region, $\vec{q} \simeq 0$. For real photons ($\vec{\epsilon} \cdot \vec{k} = 0$, with $\vec{\epsilon}$ the photon polarization vector) the S-wave photoproduction amplitude can be expressed in terms of two multipoles as,

$$\begin{aligned} \mathcal{M}_d = & 16i\pi(m_d + M_\pi) \int d^3p \phi_f^*(\vec{p}) \left\{ \mathcal{M}_1 \frac{1}{2}(\vec{\sigma}_1 + \vec{\sigma}_2) \cdot \vec{\epsilon} \right. \\ & \left. + \mathcal{M}_2 \frac{1}{2} [i \vec{\sigma}_1 \cdot \hat{k} \vec{\sigma}_2 \cdot (\vec{\epsilon} \times \hat{k}) + (1 \leftrightarrow 2)] \right\} \phi_i(\vec{p} - \vec{k}/2). \end{aligned} \quad (4)$$

The differential cross section at threshold takes the form (see appendix A)

$$\left. \frac{|\vec{k}|}{|\vec{q}|} \frac{d\sigma}{d\Omega} \right|_{|\vec{q}|=0} = \frac{8}{3} E_d^2. \quad (5)$$

In what follows, we will discuss the chiral expansion of the dipole amplitude E_d . In appendix A we discuss the relation to the commonly used amplitudes treating the deuteron as an elementary particle.

3.2 Single scattering contribution

The single scattering contribution is given by all diagrams where the photon and the pion are absorbed and emitted, respectively, from one nucleon with the second nucleon acting as a spectator (the so-called impulse approximation). One only has a contribution to the \mathcal{M}_1 amplitude of the form

$$\begin{aligned} E_d^{ss} = & \frac{1 + M_\pi/m}{1 + M_\pi/m_d} \left\{ \frac{1}{2} (E_{0+}^{\pi^0 p} + E_{0+}^{\pi^0 n}) \int d^3p \phi_f^*(\vec{p}) \vec{\epsilon} \cdot \vec{J} \phi_i(\vec{p} - \vec{k}/2) \right. \\ & \left. - \frac{k}{m} \hat{k} \cdot \int d^3p \hat{p} \frac{1}{2} (P_1^{\pi^0 p} + P_1^{\pi^0 n}) \phi_f^*(\vec{p}) \vec{\epsilon} \cdot \vec{J} \phi_i(\vec{p} - \vec{k}/2) \right\}, \end{aligned} \quad (6)$$

evaluated at the threshold value

$$|\vec{k}| = k_{\text{thr}} = M_{\pi^0} - \frac{M_{\pi^0}^2}{2m_d} = 130.1 \text{ MeV}, \quad (7)$$

and with $\vec{J} = (\vec{\sigma}_1 + \vec{\sigma}_2)/2$. A number of remarks concerning Eq.(6) are in order. It is important to differentiate between the $\pi^0 d$ and the $\pi^0 N$ ($N = p, n$) center-of-mass (COM) systems. At threshold in the former, the pion is produced at rest, it has, however, a small three-momentum in the latter [18]. Consequently, one has a single-nucleon P-wave contribution proportional to the elementary amplitudes $P_1^{\pi^0 p}$ and $P_1^{\pi^0 n}$ as defined in [15]. We use the P-wave low-energy theorems found in that paper,

$$P_1^{\pi^0 p} = 0.480 |\vec{q}| \text{ GeV}^{-2} \quad P_1^{\pi^0 n} = 0.344 |\vec{q}| \text{ GeV}^{-2}, \quad (8)$$

with

$$\vec{q} = \mu (1 - \mu) \vec{p} - \mu^2 m (1 - 5\mu/4) \hat{k}/2 , \quad (9)$$

with $\mu = M_\pi/m$ and \vec{p} is the nucleon three-momentum in the $\pi^0 d$ COM system. The derivation of Eq.(9) is sketched in appendix B. We have checked that dropping the terms of order M_π^2 in Eq.(9) does not alter the results within the precision given. Furthermore, we neglect the energy dependence of the elementary $\pi^0 p$ and $\pi^0 n$ S- and P-wave amplitudes since the pion energy changes only by 0.4% for typical average nucleon momenta in the deuteron (see appendix B). We take for the elementary S-wave pion production amplitudes the predictions from the $\mathcal{O}(q^4)$ chiral perturbation theory calculation [16],

$$E_{0+}^{\pi^0 p} = -1.16 \times 10^{-3}/M_{\pi^+} , \quad E_{0+}^{\pi^0 n} = +2.13 \times 10^{-3}/M_{\pi^+} . \quad (10)$$

In that calculation, the dominant isospin breaking effect, namely the charged to neutral pion mass difference, which is almost entirely of electromagnetic origin, has been taken into account. A fully consistent calculation including all effects from virtual photons and the quark mass differences is not yet available. The result for $E_{0+}^{\pi^0 n}$ is based on the assumption that the counter terms entering at order q^4 are the same for the proton and the neutron apart from trivial isospin factors (for a detailed discussion, see ref.[15]). We also note that only the first process has been measured, the recent determinations from MAMI and SAL give

$$E_{0+}^{\pi^0 p} = (-1.31 \pm 0.08) \times 10^{-3}/M_{\pi^+}[3] , \quad E_{0+}^{\pi^0 p} = (-1.32 \pm 0.08) \times 10^{-3}/M_{\pi^+}[4] . \quad (11)$$

Furthermore, the P-wave LET for neutral pion production off protons has been shown to hold within 3% in Ref.[3]. Using the Argonne V18 [22], the Reid soft core (RSC) [23], the Nijmegen [24] and the Paris [25] potential, we evaluate E_d^{ss} and find

$$E_d^{ss} = 0.36 \times 10^{-3}/M_{\pi^+} , \quad (12)$$

with an uncertainty of $\delta E_d^{ss} = 0.05 \times 10^{-3}/M_{\pi^+}$ due to the various potentials used. The P-wave contribution amounts to a 3% correction to the one from the S-wave, i.e. it amounts to a minor correction. The sensitivity of the single-scattering contribution E_d^{ss} to the elementary neutron- π^0 amplitude is given by

$$E_d^{ss} = 0.36 - 0.38 \cdot (2.13 - E_{0+}^{\pi^0 n}) , \quad (13)$$

all in units of $10^{-3}/M_{\pi^+}$. Consequently, for $E_{0+}^{\pi^0 n} = 0$, we have $E_d^{ss} = -0.45$ which is of opposite sign to the value based on the chiral perturbation theory prediction for $E_{0+}^{\pi^0 n}$. If one were to use the empirical value for the proton amplitude, the single-scattering contribution would be somewhat reduced.

Finally, we remark that the single-scattering contribution given in ref.[14] is very different. This is due to the following. First, in that paper a factorized form for the single-scattering contribution was used,

$$E_d^{ss} = \frac{1 + M_\pi/m}{1 + M_\pi/m_d} \frac{1}{2} (E_{0+}^{\pi^0 p} + E_{0+}^{\pi^0 n}) S_d(k_{\text{thr}}/2) = 0.41 \times 10^{-3}/M_{\pi^+}, \quad (14)$$

where $S_d(k_{\text{thr}}/2)$ is the deuteron form-factor,

$$S_d(k_{\text{thr}}/2) = \int d^3 p \phi_f^*(\vec{p}) \phi_i(\vec{p} - \vec{k}_{\text{thr}}/2) = 0.79. \quad (15)$$

Note that the isospin factor 1/2 was inadvertently omitted in [14]. Such a form is strictly correct only for the S-wave part of the deuteron wave function. Switching off the D-wave component of the deuteron wave function, we get the same result as in [14]. The main reason for the large numerical difference of our single-scattering contribution to theirs can be traced back to the use of the then accepted empirical value of $E_{0+}^{\pi^0 p} = (-2.1 \pm 0.2) \times 10^{-3}/M_{\pi^+}$ and the one from the incomplete low-energy theorem for $\gamma n \rightarrow \pi^0 n$, $E_{0+}^{\pi^0 n} \simeq 0.5 \times 10^{-3}/M_{\pi^+}$ in [14].

3.3 Three-body contributions at order q^3 ($\nu \leq -1$)

Although the $\mathcal{O}(q^3)$ (corresponding to the counting index $\nu = -2$ and -1) three-body contributions (meson exchange currents) have been worked out in ref.[14], we will give them here for completeness. In the Coulomb gauge ($\epsilon \cdot v = 0$, with v_μ the nucleons' four-velocity) and at threshold, only the two diagrams shown in Fig. 1 contribute. In momentum space, the corresponding structures are

$$a : \frac{1}{\vec{q}^2}, \quad b : \frac{(q-k)_i q_j}{[(\vec{q}-\vec{k})^2 + M_\pi^2] \vec{q}^2}, \quad (16)$$

where $\vec{q} = \vec{p} - \vec{p}'$ with \vec{p} and \vec{p}' the nucleon cms three-momenta in the initial and the final state, respectively. These expressions can be Fourier transformed into coordinate space easily and one finds that they give a contribution to the \mathcal{M}_1 amplitude defined in Eq.(4) [14]. Evaluating these with standard deuteron wavefunctions gives,

$$E_d^{(i)} = E_d^{(i,S)} + E_d^{(i,SD)} + E_d^{(i,D)} \quad (i = a, b) \quad (17)$$

where the indices S, SD, D refer to the contribution from the S-wave, the mixed and the D-wave part of the deuteron wavefunction. We find for the three-body (tb) contribution at order q^3

$$E_d^{tb,3} = (-1.90, -1.88, -1.85, -1.88) \times 10^{-3}/M_{\pi^+}, \quad (18)$$

for the Argonne V18, RSC, super soft core (SSC) [26] and Bonn potential [27] [28], in order, and using $g_A = 1.32$ as determined from the Goldberger-Treiman relation (for

$g_{\pi N} = 13.4$) (to be consistent with the calculation of the elementary amplitudes [16]). Note that we use the full (energy-dependent) model of ref.[27] throughout. The number for the Bonn potential differs from the one given in ref.[14] for three reasons. First, the overall sign of the contribution from graph b was incorrectly given and second, we find that the SD- and D-wave contributions from this graph substantially alter the pure S-wave contribution. Also, the D-wave contributions to graphs a and b were incorrectly evaluated (the corrected formulae are given in appendix C). If we, however, only retain the S-wave part of the deuteron wavefunction, we recover the result of Eq.(26) of ref.[14] (modulo the sign and within the numerical precision).

3.4 Three-body contributions at order q^4 ($\nu = 0$)

At this order, we have to consider tree graphs with exactly one insertion from the (chiral) dimension two pion-nucleon Lagrangian, which has the general form (in the isospin limit $m_u = m_d$)

$$\begin{aligned} \mathcal{L}_{\pi N}^{(2)} = & \bar{H} \left\{ -\frac{1}{2m} D^2 + \frac{1}{2m} (v \cdot D)^2 + \frac{i g_A}{2m} \{v \cdot A, S \cdot D\} \right. \\ & - \frac{i}{4m} [S_v^\mu, S_v^\nu] \left[(1 + \kappa_v) f_{\mu\nu}^+ + \frac{1}{2} (\kappa_s - \kappa_v) \text{Tr}(f_{\mu\nu}^+) \right] \\ & \left. + c_1 \text{Tr}(\chi_+) + \left(c_2 - \frac{g_A^2}{8m} \right) (v \cdot u)^2 + c_3 u \cdot u + \left(c_4 + \frac{1}{4m} \right) [S^\mu, S^\nu] u_\mu u_\nu \right\} H, \end{aligned} \quad (19)$$

where m is the nucleon mass and $f_{\mu\nu}^+ \equiv e(\xi^\dagger Q \xi + \xi Q \xi^\dagger) F_{\mu\nu}$. $F_{\mu\nu}$ is the electromagnetic field strength tensor and S^μ is the covariant spin-operator. H denotes the large component of the nucleon spinor (for more details, see ref.[5]). The terms in $\mathcal{L}_{\pi N}^{(2)}$ fall into two classes, the first one with fixed coefficients due to Lorentz invariance[7] and the second one with low-energy constants c_1, \dots, c_4 and two other constants that are directly related to the isoscalar and isovector nucleon anomalous magnetic moments, $\kappa_v = \kappa_p - \kappa_n$, $\kappa_s = \kappa_p + \kappa_n$. The pertinent three-body interaction diagrams are shown in Fig. 2, the blob characterizing an insertion from $\mathcal{L}_{\pi N}^{(2)}$. In principle, all the terms appearing in Eq.(19) can contribute. In addition, there are the recoil corrections to the graphs in Fig. 1.

Consider first insertions proportional to the low-energy constants $c_{1,2,3,4}$. One can show that all of corresponding terms vanish at threshold either due to the selection rule $S \cdot q = 0$ or due to some isospin factor of the type $\delta^{a3} \epsilon^{a3b}$. We are thus left with insertions from the terms $\sim 1/2m$, $\sim g_A/2m$ and $\sim \kappa_{v,s}$. All of these can be classified in momentum space according to the following structures,

$$\begin{aligned} & \frac{1}{\vec{q}^2}, \quad \frac{q_i}{\vec{q}^2}, \quad \frac{q_i q_j}{\vec{q}^2}, \quad \frac{q_i (p + p')_j}{\vec{q}^2}, \quad \frac{(q - k)_i (p + p')_j}{[(\vec{q} - \vec{k})^2 + M_\pi^2]}, \\ & \frac{(q - k)_i q_j}{[(\vec{q} - \vec{k})^2 + M_\pi^2]}, \quad \frac{(q - k)_i q_j (\vec{p}^2 - \vec{p}'^2)}{[(\vec{q} - \vec{k})^2 + M_\pi^2] \vec{q}^2}, \quad \frac{(q - k)_i}{[(\vec{q} - \vec{k})^2 + M_\pi^2]}, \\ & \frac{(q - k)_i q_j}{[(\vec{q} - \vec{k})^2 + M_\pi^2]^{3/2}}, \quad \frac{(q - k)_i (q - k)_j}{[(\vec{q} - \vec{k})^2 + M_\pi^2]^{3/2}}. \end{aligned} \quad (20)$$

All these operators can straightforwardly be transformed into coordinate space and the angular integrations can be performed analytically leading to the form given in Eq.(4) and one is left with one simple radial integration. Only the second operator in the second line is more easily evaluated in momentum space. Whenever possible, we have performed both types of integration as a check on our numerics (for details, see appendix C). In fact, there is a technical problem with the contribution from graphs b, l and p. Counting powers of momenta, one sees that they are divergent. This is due to the fact that in the chiral expansion one has truncated the pion–nucleon form factor and thus does not suppress the high–momentum components. This phenomenon also occurs in the calculation of the NN potential in chiral perturbation theory [10]. As it was done there, we introduce an additional Gaussian cut–off factor of the form

$$F(\vec{q}^2) = \exp\{-\vec{q}^2/\Lambda_\pi^2\} , \quad (21)$$

where the cut–off Λ_π varies between the mass of the ρ and $4\pi F_\pi = 1.2 \text{ GeV}$ (since it can be related to the mass scale of the heavy particles that are integrated out from the effective theory). Notice that the divergencies appearing in other graphs all cancel and thus no further regularization is needed for those. For energy–independent NN potentials as used here, the contribution from the graphs $n + r$ should be omitted for the reasons explained in detail in ref.[14]. We will, however, also calculate their contribution to get a very rough estimate of some of the uncertainties due to higher order graphs. Furthermore, we remark that the kinematical $1/m$ corrections to graph 1a vanish and the ones for graph 1b are taken care of by shifting the value of k_{thr} as given in Eq.(7). Finally, appendix D contains some details on calculating the time–ordered diagrams in the heavy baryon approach.

We find for the three–body (tb) contribution at order q^4

$$E_d^{tb,4} = (-0.25 , -0.23 , -0.27) \times 10^{-3}/M_{\pi^+} , \quad (22)$$

for the V18, Reid and SSC potentials, in order, and setting $\Lambda_\pi = 1 \text{ GeV}$. These amount to corrections of the order of 15% to the q^3 three–body terms. If one varies the cut–off Λ_π from 0.65 to 1.5 GeV, the three–body contribution using the V18 potential varies between -0.24 and -0.29 (in canonical units), which is a modest cut–off dependence. The result Eq.(22) is comforting since it shows that the chiral expansion of the three–body contributions is well under control. Finally, we remark that if one were to include the contribution from the recoil graphs $n + r$, the numbers given in Eq.(22) would change by less than 5 per mille.

3.5 Contribution from four–nucleon operators ($\nu = 0$)

In the $\mathcal{O}(q^3)$ calculation of ref.[14], no four–nucleon operators contributed to the deuteron electric dipole amplitude. Using Eq.(2), we see that for $\nu = 0$ we can have exactly one insertion from $\mathcal{L}_{NN}^{(1)}$. In Fig. 3a,b, we show the two graphs which in principle can contribute to pion photoproduction at threshold. Clearly, diagram 3a is only relevant for charged pion photoproduction. Graph 3b also vanishes for neutral pions, as the following argument shows. This diagram stems from the one shown in Fig. 3c by applying minimal substitution. The latter one contains the pion covariant derivative, $\vec{\nabla}_\mu = \partial_\mu \vec{\pi}/F_\pi + \dots$ which upon minimal substitution takes the form

$$\partial_\mu \pi_a \rightarrow \partial_\mu \pi_a - i e \mathcal{A}_\mu Q_{ab} \pi_b , \quad (23)$$

with

$$Q_{ab} = i \epsilon_{ab3} , \quad (24)$$

the pion charge matrix and \mathcal{A}_μ the photon field. Consequently, $\partial_\mu \pi_3 \rightarrow \partial_\mu \pi_3$ and this type of term can only contribute to charged pion photoproduction. We therefore conclude that for threshold neutral pion photoproduction to order q^4 (or up to counting index $\nu = 0$) there is *no* contribution from any four–nucleon operator and thus no new, a priori undetermined coupling constants appear. In the case of charged pion photoproduction, this would be different.

4 Results and discussion

Since as we have shown in the previous sections, neither the single scattering nor the three–body corrections depend on the potential chosen, we will present here results based on the Argonne V18 potential. The chiral expansion of the electric dipole amplitude E_d takes the form

$$\begin{aligned} E_d &= E_d^{ss} + E_d^{tb,3} + E_d^{tb,4} \\ &= (0.36 - 1.90 - 0.25) \times 10^{-3}/M_{\pi^+} = (-1.8 \pm 0.2) \times 10^{-3}/M_{\pi^+} . \end{aligned} \quad (25)$$

It is difficult to estimate the theoretical uncertainty, the value given in Eq.(25) being an educated guess, obtained as follows. We allow $E_{0+}^{\pi^0 p}$ to vary between $-1.$ and $-1.5,$ so that for a fixed value of $E_{0+}^{\pi^0 n} = 2.13,$ E_d^{ss} varies between 0.2 and 0.4 (all numbers in canonical units). The results for the three–body contributions are stable at order $q^3,$ where as we assign a conservative uncertainty of ± 0.1 to the corrections at next order due to the cut–off dependence. Clearly, this estimate does not include contributions from higher order effects, which might give rise to a larger uncertainty. Our final value is considerably smaller than the q^3 estimate reported in [14] for the reasons given above. To see the sensitivity to the elementary neutron– π^0 amplitude, we set the latter to zero and

find $E_d = -2.6 \times 10^{-3}/M_{\pi^+}$ (V18 potential) which is considerably different from the chiral perturbation theory prediction, Eq.(25), i.e. the S–wave cross section would differ by a factor of two. For other values of $E_{0+}^{\pi^0 n}$, E_d can be calculated from Eq.(13). Obviously, the sensitivity to the neutron amplitude is sizeable and is not completely masked by the larger charge–exchange amplitude as it is often stated.

On the experimental side, neutral pion photoproduction off deuterium was studied by a group at Saclay [29] and later reanalyzed in ref.[30]. In these papers, the S–wave amplitude \mathcal{E}_2 was extracted. We remark that this analysis relies heavily on the input from the elementary $\pi^0 p$ amplitude (to determine an unknown normalization factor) and therefore should only be considered indicative. The S– and P–wave multipoles used in [30] are roughly consistent with the new determinations from Mainz and Saskatoon. The amplitude \mathcal{E}_2 is related to our E_d via

$$|E_d|^2 = |\mathcal{E}_2|^2 \frac{1}{4} S_d^2 \left(\frac{1 + M_\pi/m}{1 + M_\pi/2m} \right)^2 . \quad (26)$$

Using $S_d = 0.79$ and the value of $\mathcal{E}_2 = (-4.1 \pm 0.4) \times 10^{-3}/M_{\pi^+}$ [30], we have as the “empirical” value

$$E_d^{\text{exp}} = (-1.7 \pm 0.2) \times 10^{-3}/M_{\pi^+} , \quad (27)$$

taking the same sign as given for \mathcal{E}_2 . Since we could not trace back what the exact value of S_d used in the Saclay analysis was, we took the value based on the modern potentials evaluated above. Notice that in the older papers of the Saclay group, a larger value of \mathcal{E}_2 was obtained, based on different input for the proton amplitude (which is at variance with the new data from Mainz and Saskatoon). This was used to deduce the empirical number quoted in [14]. Obviously, this experiment should be redone at a 100% duty cycle tagged photon facility, with the same accuracy as was done for the process $\gamma p \rightarrow \pi^0 p$ at MAMI and SAL and with a refined theoretical analysis as is available now. The empirical number Eq.(27) agrees nicely with the theoretical one, Eq.(25). However, we remind the reader about all the assumptions going into the extraction of this “experimental value”. Clearly, only a more precise experimental determination of E_d can tell whether this agreement is of significance. On the other hand, if one would find a discrepancy, one would either have to reassess the calculation of the elementary amplitudes by including dynamical isospin–breaking effects and/or study in more detail the wave function dependence of the order q^4 three–body corrections. Finally, two more remarks are in order. First, the sensitivity to the neutron amplitude has recently been studied in more conventional approaches [31][32]. Second, an experiment has been approved at the Mainz Microtron [33] to measure the threshold cross section for coherent neutral pion electroproduction off deuterium at a photon virtuality of $k^2 = -0.075 \text{ GeV}^2$.

Acknowledgements

VB and UGM are grateful to the Nuclear Theory Group at Argonne National Laboratory for hospitality while part of this work was completed. This research was supported in part by the U. S. Department of Energy, Nuclear Physics Division (grants DE-FG05-90ER40592 (SRB), DE-FG02-93ER-40762 (SRB), W-31-109-ENG-38 (TSHL) and DE-FG06-88ER40427 (UvK)), by NATO Collaborative Research Grant 950607 (VB, TSHL, UGM) and by the Deutsche Forschungsgemeinschaft (grant ME 864/11-1 (UGM)).

A Invariant amplitudes for the deuteron

If one considers the deuteron as an elementary particle, the S-wave photoproduction amplitude can be written as

$$\mathcal{M}_d = 8\pi(m_d + M_\pi) 2i \vec{\epsilon} \cdot \vec{J} E_d + \mathcal{O}(q) , \quad (\text{A.1})$$

with m_d the deuteron mass and $\vec{J} = \vec{L} + \vec{S}$ the deuteron *total* angular momentum, not simply the sum of the proton and the neutron spin operators. This is the form commonly used in analysing the data. Following the conventions used in [14], the slope of the differential cross section at threshold takes the form

$$\begin{aligned} \left. \frac{|\vec{k}|}{|\vec{q}|} \frac{d\sigma}{d\Omega} \right|_{|\vec{q}|=0} &= \frac{1}{64\pi^2} \frac{|\overline{\mathcal{M}_d}|^2}{(\sqrt{m_d^2 + M_{\pi^0}^2} + |\vec{k}|) (m_d + M_{\pi^0})} \\ &\simeq \frac{1}{64\pi^2} \frac{|\overline{\mathcal{M}_d}|^2}{(m_d + M_{\pi^0})^2} . \end{aligned} \quad (\text{A.2})$$

Summing over the final and averaging over the initial states leads to

$$\begin{aligned} \left. \frac{|\vec{k}|}{|\vec{q}|} \frac{d\sigma}{d\Omega} \right|_{|\vec{q}|=0} &= \frac{2}{2J+1} \sum_{M, M', \lambda} | \langle JM' | \vec{\epsilon}_\lambda \cdot \vec{J} | JM \rangle E_d |^2 \\ &= \frac{2}{2J+1} \frac{4}{3} (2J+1) |E_d|^2 = \frac{8}{3} |E_d|^2 \end{aligned} \quad (\text{A.3})$$

where M, M' are magnetic quantum numbers and λ the helicity index of the photon. We have made use of the Wigner–Eckhardt theorem and the fact that $\langle J || \vec{J} || J \rangle = \sqrt{2}$ for the deuteron.

B Two-body to three-body center-of-mass

In this appendix we sketch the derivation of the transformation from the γ - d center-of-mass (COM) system to the γ - N COM. We are interested in the kinematics of the process $\gamma N_1 N_2 \rightarrow \pi N_1 N_2$, where the nucleons, N_1 and N_2 , are sewn to the deuteron wavefunctions. Our 3-body corrections are evaluated in the γ - d COM whereas the single scattering corrections which take into account the scattering of the photon on the individual nucleons have been calculated in the γ - N COM. It is therefore necessary to construct the Lorentz transformation which boosts the single-scattering corrections to the γ - d COM.

We label energy-momenta as p_1, p_2 and k for N_1, N_2 and γ in the initial state, respectively, and p'_1, p'_2 and q for N_1, N_2 and π in the final state, respectively. The energy-momentum of the deuteron is given by $p_\psi = p_1 + p_2$ and $p'_\psi = p'_1 + p'_2$ in the initial and final state, respectively. The Fermi momentum, \vec{p} , can then be defined by $\vec{p}_1 = \vec{p}_\psi/2 + \vec{p}$

and $\vec{p}_2 = \vec{p}_\psi/2 - \vec{p}$. Note that with this labelling the initial deuteron wavefunction has the argument $(\vec{p}_1 - \vec{p}_2)/2 = \vec{p}$.

The γ - d COM is defined by $\vec{p}_\psi + \vec{k} = 0$ and the γ - N_2 COM is defined by $\vec{p}_2 + \vec{k} = 0$. The velocity of the γ - N_2 system in the γ - d COM is

$$\vec{\beta} = \frac{\vec{p}_2 + \vec{k}}{E_{2\gamma}} \quad (\text{B.1})$$

where $E_{2\gamma} = E_2 + k$. An arbitrary four-vector, (E, \vec{p}) , in the γ - d COM is expressed in the γ - N_2 COM by the matrix equation

$$\begin{pmatrix} E^* \\ p_{\parallel}^* \end{pmatrix} = \begin{pmatrix} \gamma & -\beta\gamma \\ -\beta\gamma & \gamma \end{pmatrix} \begin{pmatrix} E \\ p_{\parallel} \end{pmatrix}. \quad (\text{B.2})$$

The *-superscript indicates the γ - N_2 COM and $\vec{p} = \vec{p}_{\perp} + p_{\parallel}\hat{\beta}$. We also have $\vec{p}_{\perp}^* = \vec{p}_{\perp}$. We can now use this transformation to find k and q in both frames. In the text we use a convention in which the initial deuteron wavefunction has argument $\vec{p} - \vec{k}/2$. Here this is achieved by the substitution $\vec{p} \rightarrow -\vec{p} + \vec{k}/2$, such that $\vec{p}_2 = \vec{p} - \vec{k}$ and $\vec{p}_1 = -\vec{p}$, since N_2 must carry all the photon momentum. At the threshold point we find

$$\begin{aligned} k_0^* &= k_0 - \vec{k} \cdot \vec{p}/m, & \vec{k}^* &= \vec{k} - (k_0/m)\vec{p}, \\ E_{\pi}^* &= E_{\pi} [1 - \vec{p}^2/(2m^2)], & \vec{q}^* &= -E_{\pi}\vec{p}/m, \end{aligned} \quad (\text{B.3})$$

where we have included the first non-vanishing $1/m$ corrections. Note that the pion energy is corrected only at order $1/m^2$. Calculating these corrections with an average nucleon momentum in the deuteron obtained by means of the uncertainty principle, $\langle \vec{p} \rangle = 46$ MeV, leads to the 0.4 % shift mentioned in the main text. Of course, such a crude estimate does not properly account for binding energy effects and should be sharpened eventually.

In the γ - N_2 COM we have the multipole decomposition

$$\frac{m}{4\pi\sqrt{s}} T \cdot \epsilon = i\vec{\sigma} \cdot \vec{\epsilon} (E_{0+} + \hat{k}^* \cdot \hat{q}^* P_1) + i\vec{\sigma} \cdot \hat{k}^* \vec{\epsilon} \cdot \hat{q}^* P_2 + (\hat{q}^* \times \hat{k}^*) \cdot \vec{\epsilon} P_3. \quad (\text{B.4})$$

In terms of the transformed variables it is straightforward to find that the S-wave multipole is modified by

$$E_{0+} \rightarrow E_{0+} - \frac{k}{m} \hat{k} \cdot \hat{p} P_1 \quad (\text{B.5})$$

where we have left out terms that vanish upon integration over the Fermi momentum, and it is understood that the argument of P_1 is a transformed pion momentum.

C Nuclear matrix elements at orders q^3 and q^4

In this appendix, we give the coordinate space representations corresponding to the diagrams shown in Fig. 2. Whenever appropriate, we combine graphs. Graph d vanishes because of isospin and e and f are proportional to $v \cdot (q - k)$ which is zero at threshold to the order we are working.

a+k+o:

$$-\frac{ieg_A}{8\pi F_\pi^3}(1-2g_A^2)\int d^3r\phi^*(r)e^{-i\frac{\vec{k}\cdot\vec{r}}{2}}O_1\left\{i\frac{\vec{k}\cdot\vec{r}}{r^3}-\frac{2}{r^2}\frac{\partial}{\partial r}\right\}\phi(r), \quad (\text{C.1})$$

b+l+p:

$$\begin{aligned} &\frac{ieg_A}{8\pi F_\pi^3}(1-2g_A^2)\left[\int d^3r\phi^*(r)e^{i\frac{\vec{k}\cdot\vec{r}}{2}}\left\{\left[-2O_1\frac{Y_1(M_\pi r)}{r^2}+2O_2\frac{Y_2(M_\pi r)}{r^3}\right]\right.\right. \\ &+\frac{i}{\pi}\int d^3r'(\vec{\sigma}_1+\vec{\sigma}_2)\cdot\vec{r}'\frac{Y_1(M_\pi r')}{r'^2}\left[\frac{\vec{\epsilon}\cdot\vec{r}}{r}\frac{-i}{|r+r'|^3}\frac{\partial}{\partial r}-3\frac{\vec{\epsilon}\cdot(\vec{r}+\vec{r}')}{|r+r'|^5}\right. \\ &\left.\left.\left.\times\left(-i\frac{(\vec{r}+\vec{r}')\cdot\vec{r}}{r}\frac{\partial}{\partial r}+\frac{(\vec{r}+\vec{r}')\cdot\vec{k}}{2}\right)\right]e^{i\vec{k}\cdot\vec{r}'}\right\}\phi(r)\right], \quad (\text{C.2}) \end{aligned}$$

c+i+j:

$$\begin{aligned} &-i\frac{5eg_A}{8\pi F_\pi^3}\left[-(1+\kappa_v)\int d^3r\phi^*(r)O_3\frac{Y_1(M_\pi r)}{r^2}e^{i\frac{\vec{k}\cdot\vec{r}}{2}}\phi(r)\right. \\ &\left.+\int d^3r\phi^*(r)e^{-i\frac{\vec{k}\cdot\vec{r}}{2}}\left\{-O_1\frac{Y_1(M_\pi r)}{r^2}+O_2\left(\frac{Y_2(M_\pi r)}{r^3}-2\frac{Y_1(M_\pi r)}{r^3}\frac{\partial}{\partial r}\right)\right\}\phi(r)\right], \quad (\text{C.3}) \end{aligned}$$

g+h:

$$-\frac{ieg_A}{4\pi F_\pi^3}\int d^3r\phi^*(r)e^{-i\frac{\vec{k}\cdot\vec{r}}{2}}\left\{-O_1\frac{1}{r^3}+O_2\left(\frac{3}{r^5}-\frac{2}{r^4}\frac{\partial}{\partial r}\right)\right\}\phi(r), \quad (\text{C.4})$$

m+q:

$$\begin{aligned} &\frac{ieg_A^3}{4\pi F_\pi^3}\left\{\int d^3r\phi^*(r)e^{-i\frac{\vec{k}\cdot\vec{r}}{2}}\left[-O_1\frac{Y_1(M_\pi r)}{r^2}+O_2\left(\frac{Y_2(M_\pi r)}{r^3}-2\frac{Y_1(M_\pi r)}{r^3}\frac{\partial}{\partial r}\right)\right]\phi(r)\right. \\ &\left.-\int d^3r\phi^*(r)\left(iO_4\frac{Y_2(M_\pi r)}{r^3}+O_3\frac{Y_1(M_\pi r)}{r^2}\right)e^{i\frac{\vec{k}\cdot\vec{r}}{2}}\phi(r)\right\}, \quad (\text{C.5}) \end{aligned}$$

n+r:

$$\frac{3eg_A^3M_\pi}{8\pi^2F_\pi^3}\int d^3r\phi^*(r)e^{i\frac{\vec{k}\cdot\vec{r}}{2}}O_4\frac{1}{r^3}\left[-\frac{\partial K_0(M_\pi r)}{\partial r}+r\frac{\partial^2 K_0(M_\pi r)}{\partial r^2}\right]\phi(r), \quad (\text{C.6})$$

with

$$\begin{aligned} Y_1(M_\pi r) &= \left(M_\pi + \frac{1}{r}\right)e^{-M_\pi r}, \\ Y_2(M_\pi r) &= \left(M_\pi^2 + \frac{3M_\pi}{r} + \frac{3}{r^2}\right)e^{-M_\pi r}, \\ K_0(M_\pi r) &= \int_0^\infty dz \frac{z \sin z}{(z^2 + M_\pi^2 r^2)^{3/2}}, \quad (\text{C.7}) \end{aligned}$$

and

$$\begin{aligned}
O_1 &= (\vec{\sigma}_1 + \vec{\sigma}_2) \cdot \vec{\epsilon}, \\
O_2 &= (\vec{\sigma}_1 + \vec{\sigma}_2) \cdot \vec{r} \vec{\epsilon} \cdot \vec{r}, \\
O_3 &= \left(\vec{\sigma}_1 \cdot \vec{r} \vec{\epsilon} \cdot (\vec{k} \times \vec{\sigma}_2) + (1 \leftrightarrow 2) \right), \\
O_4 &= \left(\vec{\sigma}_1 \cdot \vec{r} \vec{\epsilon} \cdot (\vec{r} \times \vec{\sigma}_2) + (1 \leftrightarrow 2) \right), \tag{C.8}
\end{aligned}$$

Performing the angular integrations, all the spin-dependence can be expressed in terms of the spin vectors $\vec{\sigma}_{1,2}$ and the photon three-momentum \vec{k} as given in Eq.(4). The second operator in Eq.(4) stems in part from O_2 , O_3 and O_4 . The deuteron wave function $\phi(\vec{r})$ is given by

$$\phi(\vec{r}) = \frac{1}{\sqrt{4\pi}} \left(\frac{U(r)}{r} + \frac{1}{\sqrt{8}} S_{12}(\hat{r}) \frac{W(r)}{r} \right), \tag{C.9}$$

in terms of the S- and D-wave functions $U(r)$ and $W(r)$, respectively, and

$$S_{12} = 3(\vec{\sigma}_1 \cdot \hat{r})(\vec{\sigma}_2 \cdot \hat{r}) - \vec{\sigma}_1 \cdot \vec{\sigma}_2 \tag{C.10}$$

is the tensor operator. The wave function is normalized to one, $\int_0^\infty dr (U^2 + W^2) = 1$.

For completeness, we also give the corrected version of the q^3 contributions corresponding to graphs 1a and 1b. The angular integrations are performed as outlined in ref.[14] using the corrected relation

$$S_{12}^* (\vec{J} \cdot \vec{\epsilon}) S_{12} = 4 [3(\vec{\epsilon} \cdot \hat{r})(\vec{J} \cdot \hat{r}) - 2(\vec{J} \cdot \vec{\epsilon})]. \tag{C.11}$$

This gives:

a:

$$\begin{aligned}
& -\frac{ie g_A M_\pi m}{\pi F_\pi^3} \int \frac{dr}{ra^3} \left(U^2 a^2 \sin a + \frac{1}{\sqrt{2}} U W (3 \sin a - 3a \cos a - a^2 \sin a) \right. \\
& \quad \left. + \frac{1}{2} W^2 (3 \sin a - 3a \cos a - 2a^2 \sin a) \right), \tag{C.12}
\end{aligned}$$

b:

$$\begin{aligned}
& \frac{ie g_A M_\pi m}{\pi F_\pi^3} \left[\int_0^1 dz \int dr \frac{e^{-m'r}}{rb^3} \left(U^2 b^2 \sin b + \frac{1}{\sqrt{2}} U W (3 \sin b - 3b \cos b - b^2 \sin b) \right. \right. \\
& \quad \left. \left. + \frac{1}{2} W^2 (3 \sin b - 3b \cos b - 2b^2 \sin b) \right) \right. \\
& - \int_0^1 dz \int dr Y_1(m'r) \frac{1}{b^3} (\sin b - b \cos b) \left(U + \frac{1}{\sqrt{2}} W \right)^2 \\
& \left. - \frac{3|\vec{k}|}{\sqrt{2}} \int_0^1 dz (z-1) \int dr \frac{e^{-m'r}}{b^4} \left(U W + \frac{1}{\sqrt{2}} W^2 \right) ((3-b^2) \sin b - 3b \cos b) \right], \tag{C.13}
\end{aligned}$$

with

$$a = \frac{kr}{2}, \quad b = kr \left(z - \frac{1}{2} \right), \quad m' = M_\pi \sqrt{z(2-z)}. \tag{C.14}$$

D Time orderings in heavy fermion formalism

In this appendix we establish a simple method for extracting irreducible time ordered graphs in baryon chiral perturbation theory. Consider the reducible relativistic Feynman graph shown in Fig. 4. Since there are 3 interaction vertices we expect 3! time orderings. The time ordered decomposition of Fig. 4 is displayed in Fig. 5. There are several important points to note:

- Graphs (4), (5) and (6) are $1/m$ corrections and so the sum of (1), (2) and (3) correspond to the Feynman graph of Fig. 4 evaluated in the heavy fermion formalism (HFF).
- Graphs (2) and (3) are reducible and therefore graph (1) is the irreducible subgraph that we are after.

The propagator structure of Fig. 4 is

$$\frac{i}{k^2 - M_\pi^2} \frac{i(\not{p} + m)}{p^2 - m^2} = \frac{i}{2\omega} \left(\frac{1}{k_0 - \omega} + \frac{-1}{k_0 + \omega} \right) \times \frac{i}{2E_n} \left(\frac{\gamma_0 E_n - \vec{\gamma} \cdot \vec{p} + m}{p_0 - E_n} + \frac{\gamma_0 E_n + \vec{\gamma} \cdot \vec{p} - m}{p_0 + E_n} \right) \quad (\text{D.1})$$

where $E_n = \sqrt{\vec{p}^2 + m^2}$ and $\omega = \sqrt{\vec{k}^2 + M_\pi^2}$. We are interested in positive frequency pions and nucleons and so

$$(1) + (2) \propto \frac{-1}{4\omega E_n} \left(\frac{1}{k_0 - \omega} \frac{\gamma_0 E_n - \vec{\gamma} \cdot \vec{p} + m}{p_0 - E_n} \right). \quad (\text{D.2})$$

This expression can be partial fractioned to give

$$\frac{-\gamma_0 E_n + \vec{\gamma} \cdot \vec{p} - m}{4\omega E_n} \frac{1}{k_0 + p_0 - E_n - \omega} \left(\frac{1}{k_0 - \omega} + \frac{1}{p_0 - E_n} \right). \quad (\text{D.3})$$

In order to show that the two pieces inside the parentheses are in correspondence with (1) and (2), we evaluate (1) and (2) using old-fashioned time ordered perturbation theory. Here we attach a photon and a pion line to our generic interaction vertex and focus on the distinct time slices, labelled (i) and (ii) (see Fig. 6). The rules are simple: each distinct time slice —with respect to the interaction vertices— corresponds to a single energy propagator. We find

$$(1) \propto \frac{1}{[(E_1 + E_2 + E_\gamma) - (E'_1 + \omega + E_n + E_\pi)]} \quad (i) \\ \times \frac{1}{[(E_1 + E_2 + E_\gamma) - (E'_1 + \omega + E_2 + E_\gamma)]} \quad (ii) \quad (\text{D.4})$$

$$\begin{aligned}
(2) & \propto \frac{1}{[(E_1 + E_2 + E_\gamma) - (E'_1 + \omega + E_n + E_\pi)]} & (i) \\
& \times \frac{1}{[(E_1 + E_2 + E_\gamma) - (E_1 + E_n + E_\pi)]} & (ii). \quad (D.5)
\end{aligned}$$

In relativistic notation we have $k_0 = E_1 - E'_1$ and $p_0 = E_2 - E_\gamma - E_\pi$. (Note that energy is *not* conserved at the vertices in the time ordered formalism.) It then follows that

$$\begin{aligned}
(1) & \propto \frac{1}{k_0 + p_0 - E_n - \omega} \times \frac{1}{k_0 - \omega} \\
(2) & \propto \frac{1}{k_0 + p_0 - E_n - \omega} \times \frac{1}{p_0 - E_n}. \quad (D.6)
\end{aligned}$$

We are now in position to establish a rule for extracting the irreducible time ordered subgraph, (1), in HFF. The propagator structure of Fig. 4 in HFF is

$$\frac{i}{k^2 - M_\pi^2} \frac{i}{v \cdot k} \quad (D.7)$$

where $p = mv + k$. In the static limit $v \cdot k \rightarrow k_0=0$, which renders (D.7) singular. In this limit $E_n = m$ and $p_0 = m - k_0$. Therefore, decomposing the propagators gives

$$\begin{aligned}
\frac{i}{k^2 - M_\pi^2} \frac{i}{k_0} &= \frac{i}{2\omega} \left(\frac{1}{k_0 - \omega} + \frac{-1}{k_0 + \omega} \right) \times \frac{-i}{p_0 - E_n} \\
&= \frac{1}{2\omega} \frac{1}{(k_0 - \omega)(p_0 - E_n)} + (-) T.O. \\
&= \frac{1}{2\omega} \frac{1}{k_0 + p_0 - E_n - \omega} \left(\frac{1}{k_0 - \omega} + \frac{1}{p_0 - E_n} \right) + (-) T.O. \\
&= \frac{1}{2\omega} \frac{1}{(k_0 + p_0 - E_n - \omega)} \frac{1}{(k_0 - \omega)} + \text{reducible } (+) T.O. + (-) T.O. \quad (D.8)
\end{aligned}$$

where (\pm) refers to the frequency of the time ordering and (D.6) was used in the last line. The first term is graph (1) of Fig. 5, the *irreducible* $(+)$ $T.O.$ piece. It is, of course, well behaved in the static limit. In the limit $k_0 \rightarrow 0$ we have

$$\text{irreducible } (+) T.O. = \frac{1}{2\omega^3} = \frac{1}{2(\vec{k}^2 + M_\pi^2)^{3/2}} \quad (D.9)$$

and so the irreducible time ordering in a HFF Feynman graph of type Fig. 4 can be extracted by making the following replacement in the HFF propagators:

$$\frac{i}{k^2 - M_\pi^2} \frac{i}{v \cdot k} \implies \frac{1}{2(\vec{k}^2 + M_\pi^2)^{3/2}}. \quad (D.10)$$

References

- [1] J. Gasser and H. Leutwyler, Nucl. Phys. B94, 269 (1975).
- [2] S. Weinberg, Trans. N.Y. Acad. Sci. 38, 185 (1977).
- [3] M. Fuchs et al., Phys. Lett. B368, 20 (1996).
- [4] J. Bergstrom et al., Phys. Rev. C53, R1052 (1996).
- [5] V. Bernard, N. Kaiser, and Ulf-G. Meißner, Int. J. Mod. Phys. E4, 193 (1995).
- [6] E. Jenkins and A.V. Manohar, Phys. Lett. B255, 558 (1991).
- [7] V. Bernard, N. Kaiser, J. Kambor, and Ulf-G. Meißner, Nucl. Phys. B388, 315 (1992).
- [8] S. Weinberg, Nucl. Phys. B363, 3 (1991).
- [9] S. Weinberg, Phys. Lett. B251, 288 (1990).
- [10] C. Ordóñez, L. Ray and U. van Kolck, Phys. Rev. Lett. 72, 1982 (1994); Phys. Rev. C53, 2086 (1996).
- [11] U. van Kolck, Phys. Rev. C49, 2932 (1994).
- [12] T.-S. Park, D.-P. Min and M. Rho, Phys. Rep. 233, 341 (1993).
- [13] S. Weinberg, Phys. Lett. B295, 114 (1992).
- [14] S.R. Beane, C.Y. Lee and U. van Kolck, Phys. Rev. C52, 2914 (1995).
- [15] V. Bernard, N. Kaiser and Ulf-G. Meißner, Z. Phys. C70, 483 (1996).
- [16] V. Bernard, N. Kaiser and Ulf-G. Meißner, Phys. Lett. B378, 337 (1996).
- [17] V. Bernard, N. Kaiser and Ulf-G. Meißner, Phys. Lett. B383, 116 (1996).
- [18] J.H. Koch and R.M. Woloshyn, Phys. Rev. C16, 1968 (1977).
- [19] P. Bosted and J. Laget, Nucl. Phys. A296, 413 (1978).
- [20] G. Fäldt, Phys. Scrip. 22, 5 (1980); G. Fäldt and T.E.O. Ericson, Phys. Lett. B89, 173 (1980).
- [21] S.S. Kamalov, L. Tiator and C. Bennhold, Phys. Rev. Lett. 75, 1288 (1995).
- [22] R.B. Wiringa, V.G. Stoks and R. Schiavilla, Phys. Rev. C51, 38 (1995).

- [23] R.V. Reid, Ann. Phys. (NY) 50, 411 (1968).
- [24] M.M. Nagels, T.A. Rijken and J.J. de Swart, Phys. Rev. D17, 768 (1978).
- [25] M. Lacombe et al., Phys. Rev. D12, 1495 (1975); Phys. Rev. C21, 861 (1980).
- [26] R. de Tournell and D.W. Sprung, Nucl. Phys. A210, 193 (1973).
- [27] R. Machleidt, K. Holinde, and Ch. Elster, Phys. Rep. 149, 1 (1987).
- [28] R. Machleidt, Adv. Nucl. Phys. 19, 189 (1989).
- [29] P. Argan et al., Phys. Rev. Lett. 41, 629 (1978); Phys. Rev. C24, 300 (1981).
- [30] P. Argan et al., Phys. Lett. B206, 4 (1988).
- [31] M.I. Levchuk, V.A. Petrun'kin and M. Schumacher, Z. Phys. A355, 317 (1996).
- [32] S.S. Kamalov, L. Tiator and C. Bennhold, Phys. Rev. C55, 98 (1997).
- [33] MAMI Proposal A1/1-96, Spokesperson: R. Neuhausen.

Figures

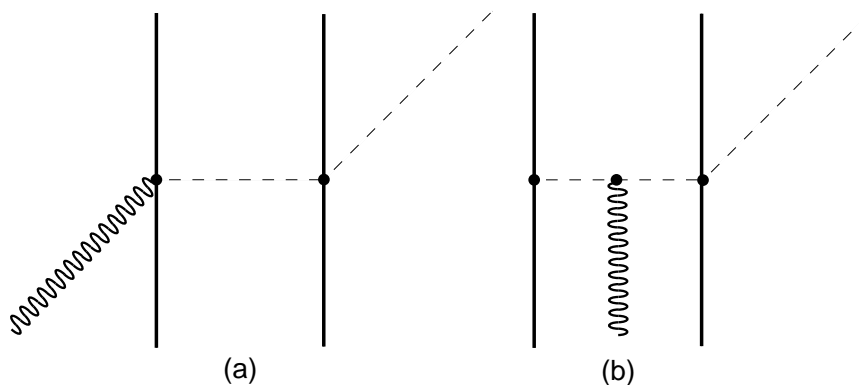
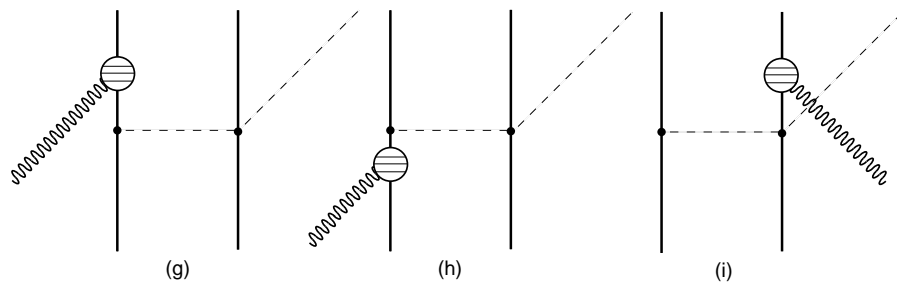
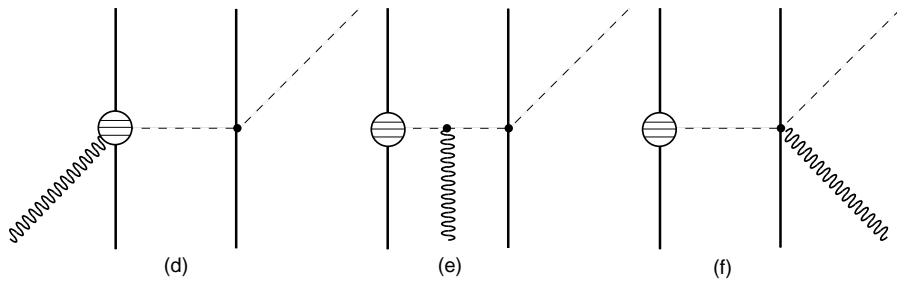
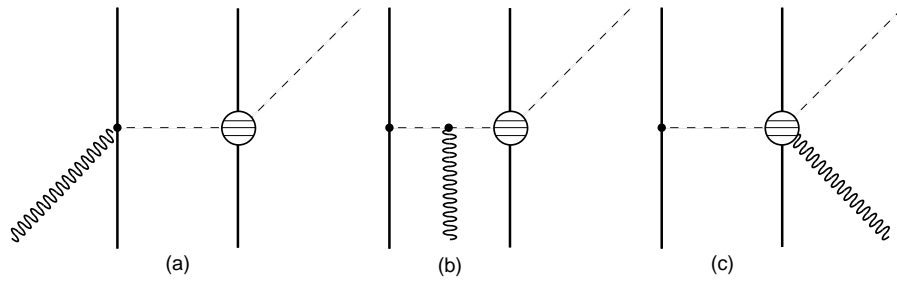


Figure 1: Three-body interactions which contribute to neutral pion photoproduction at threshold to order q^3 (in the Coulomb gauge).



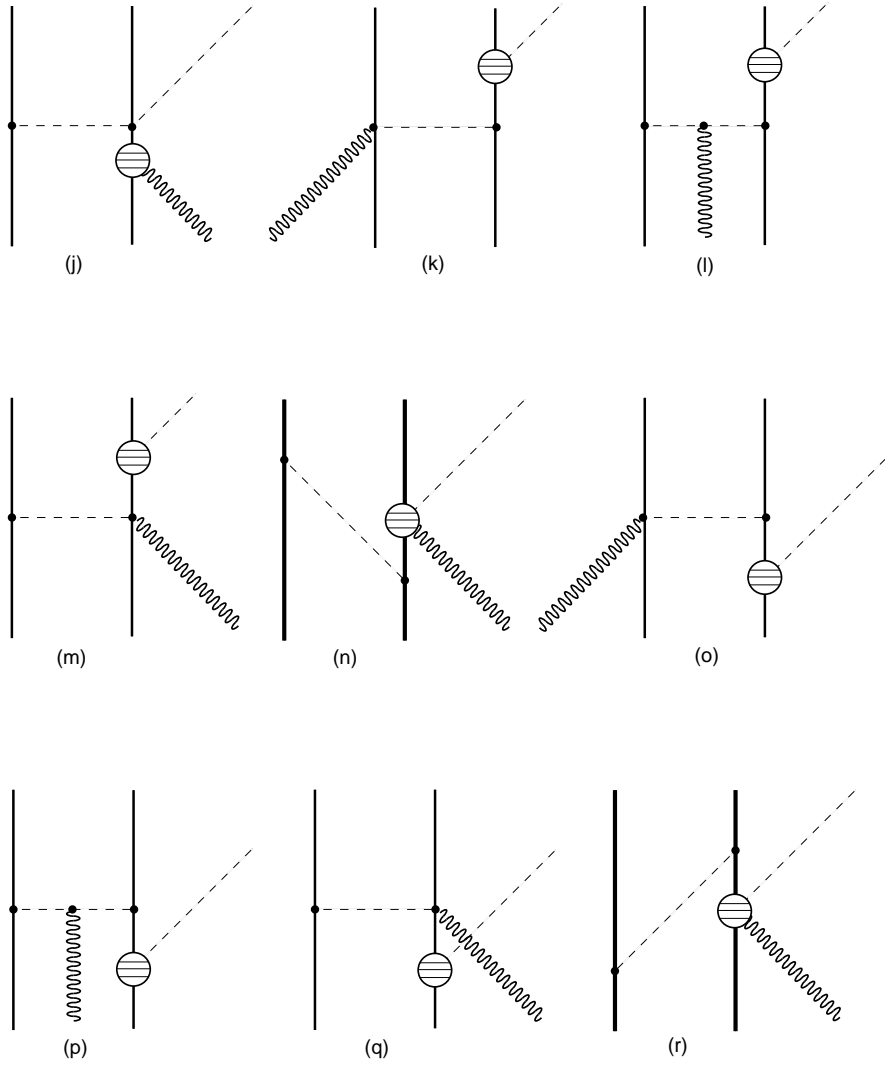


Figure 2: Graphs contributing at order q^4 to neutral pion photoproduction. The hatched circles denote an insertion from $\mathcal{L}_{\pi N}^{(2)}$. The time-ordered graphs are distinguished by bold nucleon lines.

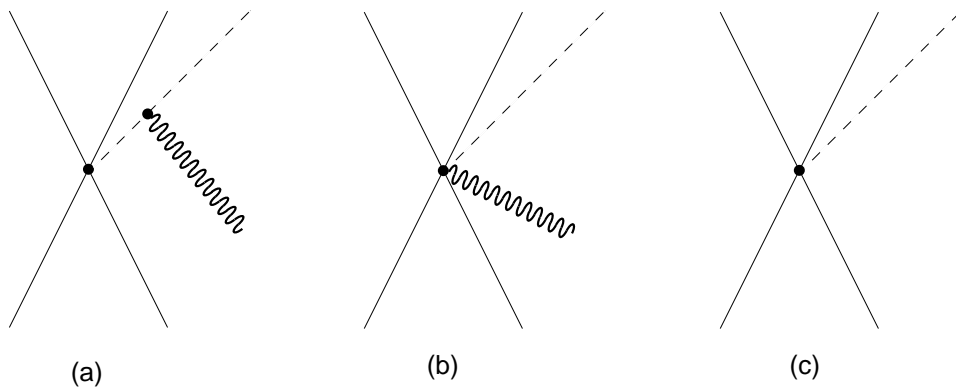


Figure 3: Four-fermion terms contributing to (charged) pion photoproduction for $\nu = 0$ (graphs a and b). Graph b is generated from graph c by minimal substitution.

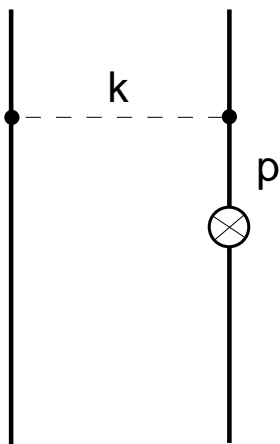


Figure 4: A two-nucleon reducible relativistic Feynman graph. The cross denotes a generic interaction vertex.

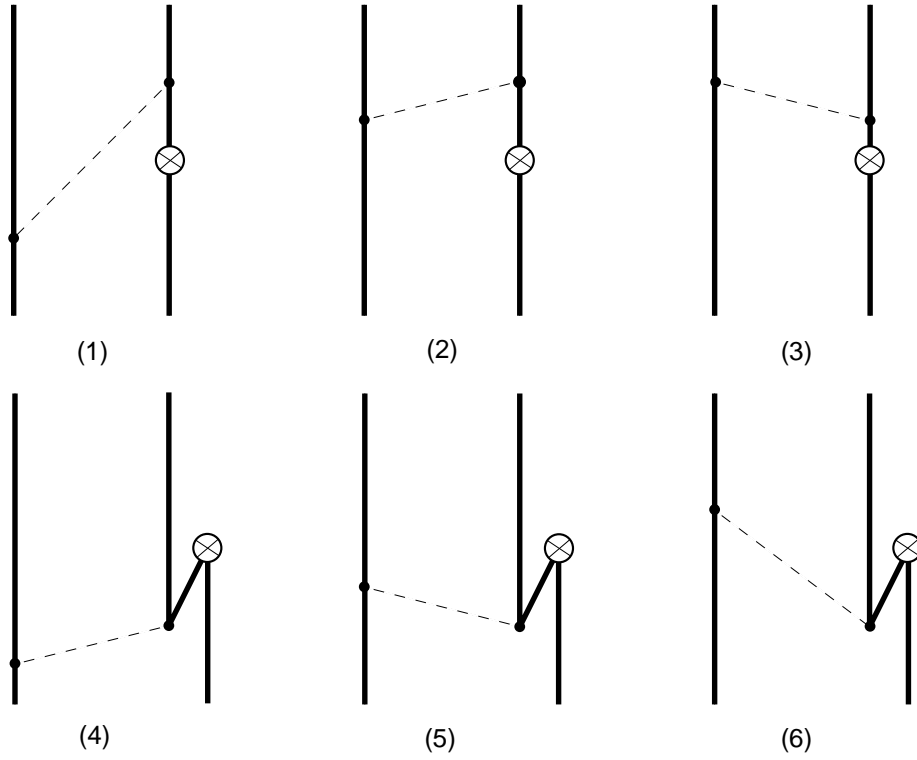


Figure 5: Decomposition of Fig. 4 into distinct time orderings. Graphs (4), (5) and (6) are $1/m$ corrections and so the sum of (1), (2) and (3) is the Feynman graph in HFF.

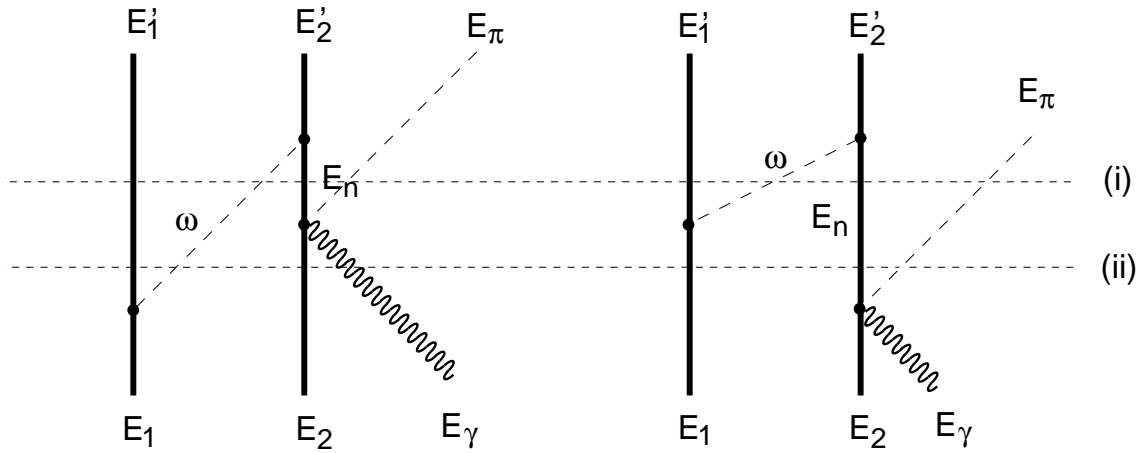


Figure 6: Time slices for graphs (1) and (2) of Fig. 5 with pion and photon attached. All energies flow from bottom to top.